

Film Tension and Film Rupture of Alkanes at the Air–Water Interface Using Axisymmetric Drop Shape Analysis

P. Chen, C. Mak, S. S. Susnar, and A. W. Neumann*

Department of Mechanical and Industrial Engineering, University of Toronto, 5 King's College Road, Toronto, Ontario, Canada M5S 3G8

Received: September 22, 1997; In Final Form: January 28, 1998

In connection with interfacial tension measurements for *n*-hexadecane–water under conditions of mutual saturation, we accidentally found an extremely high tension value for the aqueous phase of approximately 80 mJ/m², using axisymmetric drop shape analysis–profile (ADSA-P) for an air bubble formed in the water phase. This high tension value is that of an alkane film at the air–water interface. From static measurements (the drop surface area kept constant) at 25 ± 0.2 °C, we observed this film tension value to be 80.67 ± 0.06 and 77.20 ± 0.02 mJ/m² at the 95% confidence level for hexadecane and dodecane films at the air–water interface, respectively. These film tension values were also confirmed in dynamic measurements (the drop surface area continuously increased) for both alkane systems. In addition, film rupture has been demonstrated both in the sudden change in the bubble profile and in the abrupt decrease in the tension value. The alkane film tension measured is approximately equal to the sum of the interfacial tensions of air–alkane and alkane–water. The method presented provides a new way to measure film tension; it utilizes axisymmetric drops or bubbles. This is less restrictive than other approaches that require the drop or bubble to be spherical. The measurements for film tension can be carried out under both static and dynamic conditions, and information about the surface area, drop, or bubble volume as well as the radius of curvature can all be obtained simultaneously.

I. Introduction

For measuring interfacial tension between two immiscible liquids, it is necessary to ensure that the two liquids are mutually saturated.¹ This is crucial in determining the spreading coefficient for one liquid on another.^{1,2} In the case of benzene on water, the spreading coefficient determined from the surface tensions of the two pure liquids is positive, indicating spontaneous spreading, while the spreading coefficient determined from the surface tensions of the two mutually saturated liquids is negative, indicating the formation of a benzene liquid lens on water. When water is saturated with benzene, the surface contains benzene molecules, and hence the surface tension is reduced to 62.2 mJ/m² from that of pure water of 72.8 mJ/m² at 20 °C.¹ In our recent experiments on alkane–water interfacial tensions, we found that the surface tension of water saturated with alkane was indeed different from that of pure water; however, instead of finding a surface tension value that is lower than that of pure water, we observed a surface tension value that is higher than that of pure water. For water saturated with hexadecane, this tension value is approximately 80 mJ/m², compared with 72 mJ/m² for pure water, at 25 °C.

Our surface tension measurements were performed by using axisymmetric drop shape analysis–profile (ADSA-P),^{3–7} in which the surface tension was measured through drop shape analysis on an air bubble formed at the tip of a Teflon tube, inside the water phase. During the experiment, the water phase was in contact with the alkane liquid (second bulk phase) in order to ensure mutual saturation. The resulting high tension value cannot be attributed to impurities in the liquids. Since

impurities are usually hydrophobic in nature and will adsorb at the air–water interface, the presence of impurities will likely reduce the water surface tension, rather than increase it. Therefore, an alternative explanation must be sought.

It was noted that during the experiment both alkane and water were present, and the Teflon tube was moved through the alkane before it reached into the water. Thus, a small amount of alkane might have adhered to the Teflon capillary, especially near its tip area, during the process of insertion of the Teflon tube into the liquids. When forming an air bubble at the Teflon tip in the water phase by pumping air through the Teflon tube, an alkane film might be brought onto the air–water interface; i.e., an alkane film might be spread on the air–water interface. Thus, instead of measuring the air–water surface tension, we might actually have measured alkane film tension.

To confirm this proposition, we must design an experiment that will show clearly both the conditions under which film tension and surface tension are measured. It is noted that the spreading coefficient of alkanes on a water surface is negative,^{1,2} and hence an alkane film formed on the water surface is not thermodynamically stable. Thinning of such a film may eventually lead to film rupture. Therefore, we wish to design an experiment in which an alkane film formed on the surface of an air bubble is thinned by increasing the surface area. It is expected that as the film becomes sufficiently thin, any random mechanical or thermal disturbance will readily break the continuous film coverage on the air–water interface. Once the film ruptures, the surface under observation will be that of air–water, and the shape of the air bubble will be determined by the interface tension between air and water in conjunction with gravity. Hence, ADSA-P (a drop shape technique) should give a reliable value for the water surface tension.

* To whom correspondence should be addressed.

It is the purpose of this work to design an experiment that will record the dynamics of film thinning and film rupture, i.e., to develop a new methodology for measuring film tension. This is significant since, presently, compared to the number of techniques for measuring interfacial tension,¹ only a small number of methods^{8–18} have been developed for measuring film tension. All of these approaches make use of a spherical drop or bubble and relate the simple geometric parameters of the sphere to the Laplace equation of capillarity in order to calculate film tension. It is worth noting that Princen and Mason¹⁹ did describe yet another method that relies on a film at the top of a (not necessarily spherical) bubble or drop, but the top portion of the drop supporting the film is necessarily spherical. As reported by Soos et al.,¹⁷ the restriction that the drop or bubble supporting the film be spherical requires the Eötvös number^{20,21} to be below 0.02. This will restrict the use of the current techniques for measuring film tension since not all film systems can satisfy this condition and maintain spherical geometry. Our present technique can overcome this difficulty and requires only axisymmetric drop or bubble shapes.

In this paper, we report film tension measurements for two alkane systems: hexadecane and dodecane films at an air–water interface. We also confirm that the high tension value obtained from the drop shape analysis (ADSA-P) corresponds to that of a film.

II. Materials and Methods

A. Materials. The two pairs of immiscible liquids used were hexadecane–water and dodecane–water. Hexadecane and dodecane with a purity of 99+% were obtained from Aldrich Chemical Co., Inc. Water was distilled; its purity was checked by the surface tension measurement which, at 25 ± 0.2 °C, resulted in 72.14 ± 0.04 mJ/m² at the 95% confidence level. The two liquids of each pair were saturated with each other for at least 12 h before the experiment.

B. Axisymmetric Drop Shape Analysis—Profile (ADSA-P). Detailed descriptions of axisymmetric drop shape analysis—profile are given elsewhere.^{3–7} Briefly, ADSA-P fits the theoretical drop profile given by the Laplace equation to the experimentally obtained drop profile. An objective function is formed that describes the deviation of the experimental profile from the theoretical one. This function is minimized by a nonlinear least-squares regression procedure, yielding the interfacial tension or film tension. The program also provides the volume, surface area, and the radius of curvature at the apex. The program requires several randomly chosen coordinate points along the drop profile, the value of the density difference across the interface, and the magnitude of the local gravitational constant as input. Each single image of a drop is analyzed 10 times with 20 different, arbitrary profile coordinate points each time.

C. Experiment. The hardware design for film tension measurement is identical to that for interfacial tension.^{2,6} The difference is only in the procedure of sample arrangement.

1. Sample Preparation and Experimental Procedure for Measuring Film Tension. To maintain mutual saturation between alkane and water during the experiment, a special setup² was used in the sample arrangement (Figure 1). Both alkane and water were contained in a quartz cuvette (Hellma 330984, $20 \times 50 \times 80$ mm³), where a Teflon tube (capillary) of circular cross section (outer diameter 1.6 mm, inner diameter 1.0 mm) framed by a “J”-shaped stainless steel tube was inserted into the water phase initially. To ensure that a small amount of alkane adhered to the tip of the Teflon tube, the capillary was

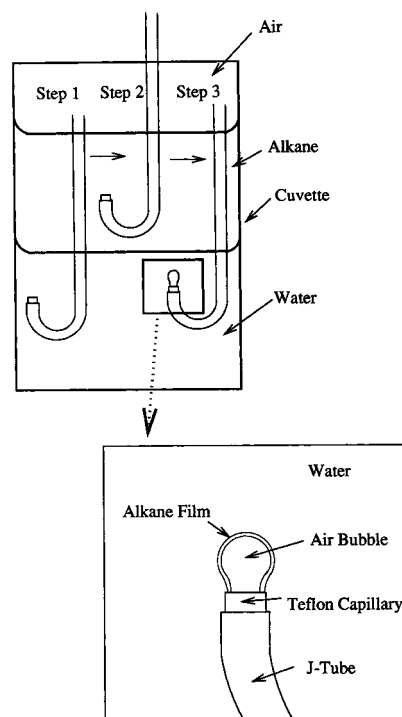


Figure 1. Experimental setup for film tension measurements. To form a film, the capillary is raised into the alkane phase by a micromanipulator positioned above the cuvette (step 1 to step 2). Then, using a microsyringe connected to the other end of the capillary, a minute amount of alkane is withdrawn into the capillary (step 2). Finally, the capillary is lowered down into the water phase, and an air bubble coated with an alkane film is formed at the tip of the capillary by pumping air through the tube slowly (step 3).

then raised into the alkane phase by a micromanipulator positioned above the cuvette. Using a microsyringe connected to the other end of the capillary, a minute amount of alkane was withdrawn into the capillary. Then, the capillary was lowered into the water phase again. Finally, an air bubble was formed at the tip of the capillary by pumping air through the capillary slowly, in the process creating an alkane film on the air bubble.

As mentioned in the Introduction, it should be possible for an alkane film to be broken by certain mechanical or thermal disturbances when it becomes sufficiently thin. Hence, the volume of the air bubble formed was increased continuously using the microsyringe; consequently, the surface area of the air bubble was increased at a rate ranging from 0.5 to 3 mm²/s. (The surface area of the air bubble was generally between 20 and 40 mm².) While the film was thinning, images of the air bubble shape were acquired at 0.3 s time intervals. The corresponding surface or film tension was calculated by ADSA-P.

2. Sample Preparation and Experimental Procedure for Measuring Interfacial Tension. To measure the interfacial tension between alkane and water, an inverted pendant alkane drop was formed at the tip of the Teflon tube immersed in the water phase. To measure their respective surface tensions, air bubbles were formed in the two liquid phases.^{2,7}

3. Experimental Setup. The setup was essentially the same as that of the usual ADSA-P.^{3–7} Briefly, for both film and interfacial tension measurements, a drop or bubble was illuminated with a white light source (model V-WLP 1000, Newport Corp., Irvine, CA) shining through a heavily frosted diffuser (Figure 2). Images of the drop were obtained by a microscope (Leitz Apozoom, Leica, Willowdale, ON, Canada)

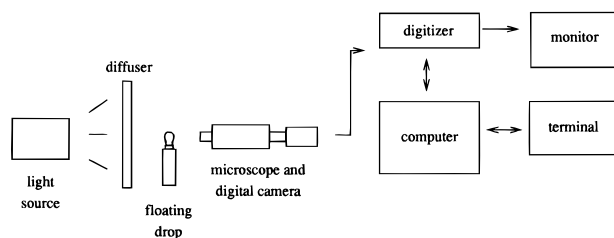


Figure 2. Schematic of the experimental setup for tension measurements using ADSA-P.

linked to a monochrome charge-coupled device video camera (Cohu 4810, Infrascan, Inc., Richmond, BC, Canada). The video signal of the drop was transmitted to a digital video processor (Xvideo board, Parallax Graphics Inc., Santa Clara, CA) which performed the frame grabbing and digitization of the image to 640×480 pixels with 256 gray levels. For each run, images were captured at 0.3 s intervals in order to observe the time-dependent film and interfacial tensions. A workstation (Sun SPARCstation 10, Sun Microsystems, Mountain View, CA) was used to acquire the images from the digitization board. Image analysis schemes were used to determine the drop profile coordinates with subpixel resolution and correct for optical distortion.^{4,5} The entire setup, except for the workstation, was placed on a vibration-free table (Technical Manufacturing Corp., Peabody, MA) to isolate the system from external disturbances (Figure 2). All the measurements reported here were conducted at room temperature of 25 ± 0.2 °C.

III. Results

For each of the two systems, both static and dynamic measurements were performed: in the former, the measurements were conducted while the air bubble volume was kept constant, and hence there was no thinning of the film; in the latter, the measurements were conducted while the air bubble volume and surface area were increased, resulting in thinning of the film. The experimental results reported were repeated on three different days; during each day multiple runs were conducted for each type of measurement, each run usually containing tens or hundreds of images. The 95% confidence limits presented below are based on a statistical analysis for all of the experiments conducted.

A. Hexadecane–Water. 1. Static Measurements. When a small amount of alkane adheres to the tip of the Teflon tube, a film can be created at the air–water interface by slowly forming the air bubble at the tip. Figure 3 shows a typical image of an air bubble coated with a hexadecane film, inside the water phase; the tension value determined by ADSA-P is 80.60 mJ/m^2 . Such a bubble can be maintained for 10 min or more, and Figure 4 shows the film tension over a time span of 5 min after the film was formed. In this figure, there is a slightly increasing trend of tension with time. By performing a linear regression, it was found that the slope of the line is $3.44 \times 10^{-4} \text{ mJ/(m}^2 \text{ s)}$, which corresponds to a tension increase of 0.2 mJ/m^2 in 10 min. Using a null hypothesis, i.e., assuming a zero slope, it follows that the trend is statistically significant, with a certainty larger than 99.9%. Presumably, the slight increase in tension is caused by film drainage due to gravity (see also the Discussion section). It is reasonable to assume that the tension would approach a plateau value asymptotically if the film could be maintained; however, the current technique cannot avoid external disturbances which cause film rupture (see also below). Considering the small increase in tension, it was decided to average the data

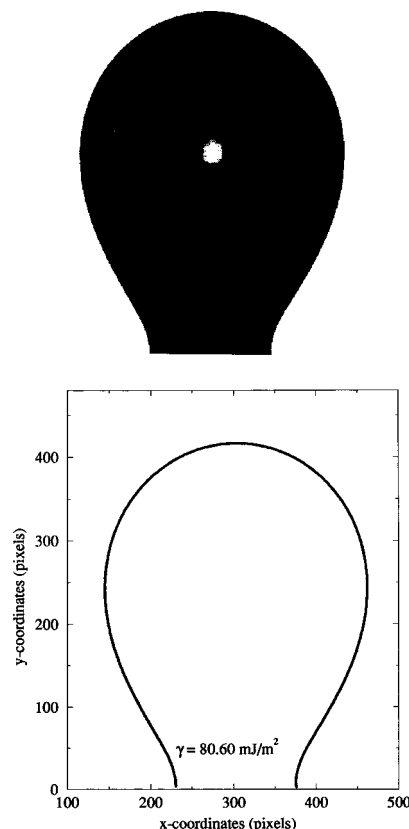


Figure 3. A typical image and its profile (bottom) of an air bubble coated with a hexadecane film, inside the water phase. The film tension analyzed by ADSA-P from this single image is 80.60 mJ/m^2 . It is noted that the profile is smooth.

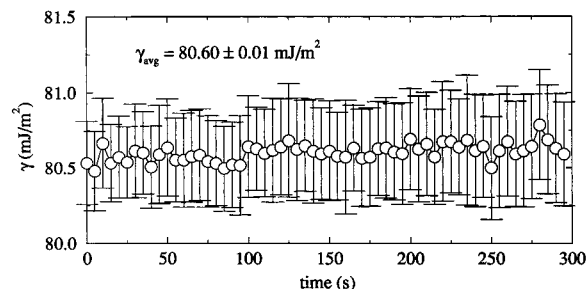


Figure 4. A typical static hexadecane film tension measurement over a time span of 5 min, which results in a film tension of $80.60 \pm 0.01 \text{ mJ/m}^2$ at the 95% confidence level.

over the entire range to represent the film tension value. The average value in Figure 4 is $80.60 \pm 0.01 \text{ mJ/m}^2$ at the 95% confidence level based on this single run; the overall average film tension calculated from ADSA-P is $80.67 \pm 0.06 \text{ mJ/m}^2$ at the 95% confidence level after taking into account four different runs. This tension value is extremely high, compared with the surface tension of pure water of about 72.14 mJ/m^2 at 25 °C.

It was expected that complete film coverage on the air–water interface could be generated only if there was a sufficient amount of alkane at the tip of the Teflon tube. Otherwise, the resulting surface of the air bubble would be water. To test this idea, the following procedure was adopted: A series of air bubbles were formed and released from the tip of the Teflon tube by continually pumping air with the microsyringe. As long as a hexadecane film forms, a certain amount of the alkane will be removed with each air bubble, gradually depleting the hexadecane “reservoir” at the tip. Consequently, a point may

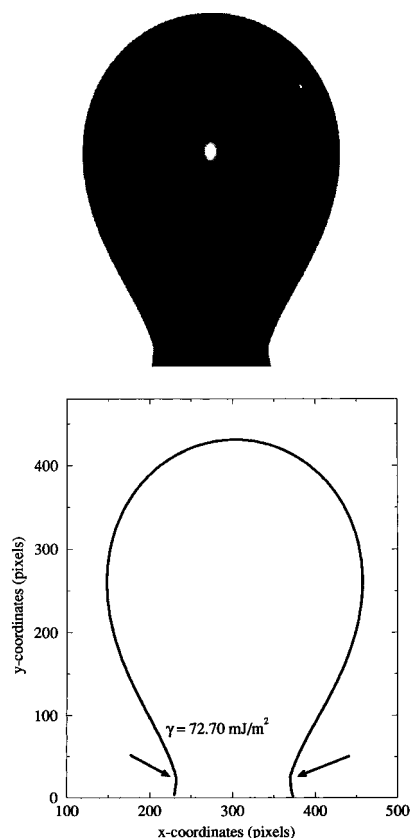


Figure 5. A typical image of an air bubble after rupture of hexadecane film and its profile. The interfacial tension from this single image is 72.70 mJ/m^2 . Note that two kinks appear in the neck region of the cross-section profile of the air bubble, as indicated by arrows, indicating the presence of a ring of hexadecane.

be reached where there is insufficient alkane to form a film. Figure 5 shows a typical image of an air bubble created under this condition. It is noted that two kinks, or discontinuity points, occur in the neck region of the bubble profile (Figure 5b). These kinks are believed to indicate a "ring" of the residual alkane accumulated at the base of the bubble; the resulting tension value is 72.70 mJ/m^2 , which is close to that of water at 25°C .

2. Dynamic Measurements. To confirm the two different tension values, shown above, resulting from the same system but different procedures (one identified as the alkane film tension and the other the interfacial tension between air and water), time-dependent tension measurements were performed: The volume of the air bubble was increased continuously by means of the motorized syringe. Three rates of the surface area increase were obtained: 3.05 , 0.61 , and $0.52 \text{ mm}^2/\text{s}$. The same initial surface area was used for all expansion rates to ensure valid comparison (see below). As the surface area is increased, film thinning occurs; one would then expect film rupture to occur at some point. Figure 6 shows such a dynamic measurement, at a surface expansion rate of $3.05 \text{ mm}^2/\text{s}$, on a single bubble; images were acquired at 0.3 s time intervals. It is seen that a transition in the bubble profile occurs at time $t = 0.64 \text{ s}$ when the drop image vibrates severely and cannot be processed by the image analysis program of ADSA-P (Figure 6a). Before the transition, static and optically "smooth" profiles are observed (Figure 6b,c). After the transition, kinks emerge in the neck region of the drop profile (Figure 6b,c) and remain throughout the experiment (lasting up to 10 min , not shown in Figure 6). When analyzing the images with ADSA-P, the tension before the transition is approximately 80.0 mJ/m^2 , and the tension after the transition is approximately

72.6 mJ/m^2 . At the transition, an abrupt change in the tension occurs, corresponding to a tension decrease of approximately 7.4 mJ/m^2 .

From Figure 6a, it is also noted that a black dot appears in the bright central area of the bubble image after the transition, at times $t = 1.55$, 3.15 , and 3.46 s . (The bright central area is caused by light that is transmitted through a relatively small area of the bubble which is essentially perpendicular to the incident light beam.) This black dot is due to a small hexadecane droplet adhering to the bubble surface, preventing the light from being transmitted. This black dot drifts down along the air–water interface with the passage of time (see images at $t = 3.15 \text{ s}$ and $t = 3.46 \text{ s}$). This indicates that, at the transition, the film ruptures into small droplets, which consequently slide down along the air–water interface due to gravity and coalesce into a "ring". This confirms the above supposition of film tension and film rupture.

Figure 7 shows the tension results over a larger time span, when the surface area is increased at a rate of $3.05 \text{ mm}^2/\text{s}$, corresponding to a bubble volume increasing at a rate of $2.12 \text{ mm}^3/\text{s}$. It is seen that, with film thinning, the film tension increases gradually up to about 80.0 mJ/m^2 when film rupture occurs; accompanying this, there is a sharp decrease in the tension value to 72.6 mJ/m^2 . After this transition, the surface tension remains constant at about 72.6 mJ/m^2 even though the surface area continues to increase at the same rate. One of the interesting features observed is the gradual increase in film tension along with the thinning of the film. A linear curve fit to these tension values results in a slope of $1.01 \pm 0.10 \text{ mJ}/(\text{m}^2 \text{ s})$ with a correlation coefficient of 0.957 (Figure 7). To relate the film tension to the thinning, the ratio of this slope to the surface expansion rate has to be calculated, which turns out to be $0.331 \text{ mJ}/(\text{m}^2 \text{ mm}^2)$. This means that the film tension increases by 0.331 mJ/m^2 for every mm^2 surface area increase. To relate this surface area increase to film thinning, the absolute value of the surface area has to be used. Therefore, as mentioned before, in our experiments the same initial surface area of the bubble was always used for different bubble expansion measurements to ensure valid comparison (see below). The purpose of drawing a straight line through the tension data in Figure 7 and subsequent figures was to allow for a comparison between different rates of surface expansion. Upon further thinning, a final tension value might well be approached asymptotically, if rupture can be prevented.

Figures 8 and 9 are dynamic film tensions recorded when the surface areas are increased at rates of 0.61 and $0.52 \text{ mm}^2/\text{s}$, respectively. Similarly, the tension value increases up to approximately 80.0 mJ/m^2 as the surface area is increased, followed by a sharp decrease in tension, corresponding to film rupture. After film rupture, the film tension drops to approximately 72.6 mJ/m^2 . A linear curve fit to the film tension values, before film rupture, results in the slopes of $0.24 \pm 0.03 \text{ mJ}/(\text{m}^2 \text{ s})$ (with a correlation coefficient of 0.869) and $0.12 \pm 0.01 \text{ mJ}/(\text{m}^2 \text{ s})$ (with a correlation coefficient of 0.834) for the two surface expansion rates of 0.61 and $0.52 \text{ mm}^2/\text{s}$, respectively (Figures 8 and 9).

Again, to relate these film tension increases to the film thinning, the ratios of these slopes to the surface expansion rates need to be calculated: 0.393 and $0.231 \text{ mJ}/(\text{m}^2 \text{ mm}^2)$ for Figures 8 and 9, respectively. These ratios are reasonably close to that calculated from Figure 7, i.e., at $0.331 \text{ mJ}/(\text{m}^2 \text{ mm}^2)$. Comparing these three ratios calculated from Figures 7–9, it is seen that the film tension seems to be related only to the film thinning, not to the rate of the surface area increase; the surface expansion

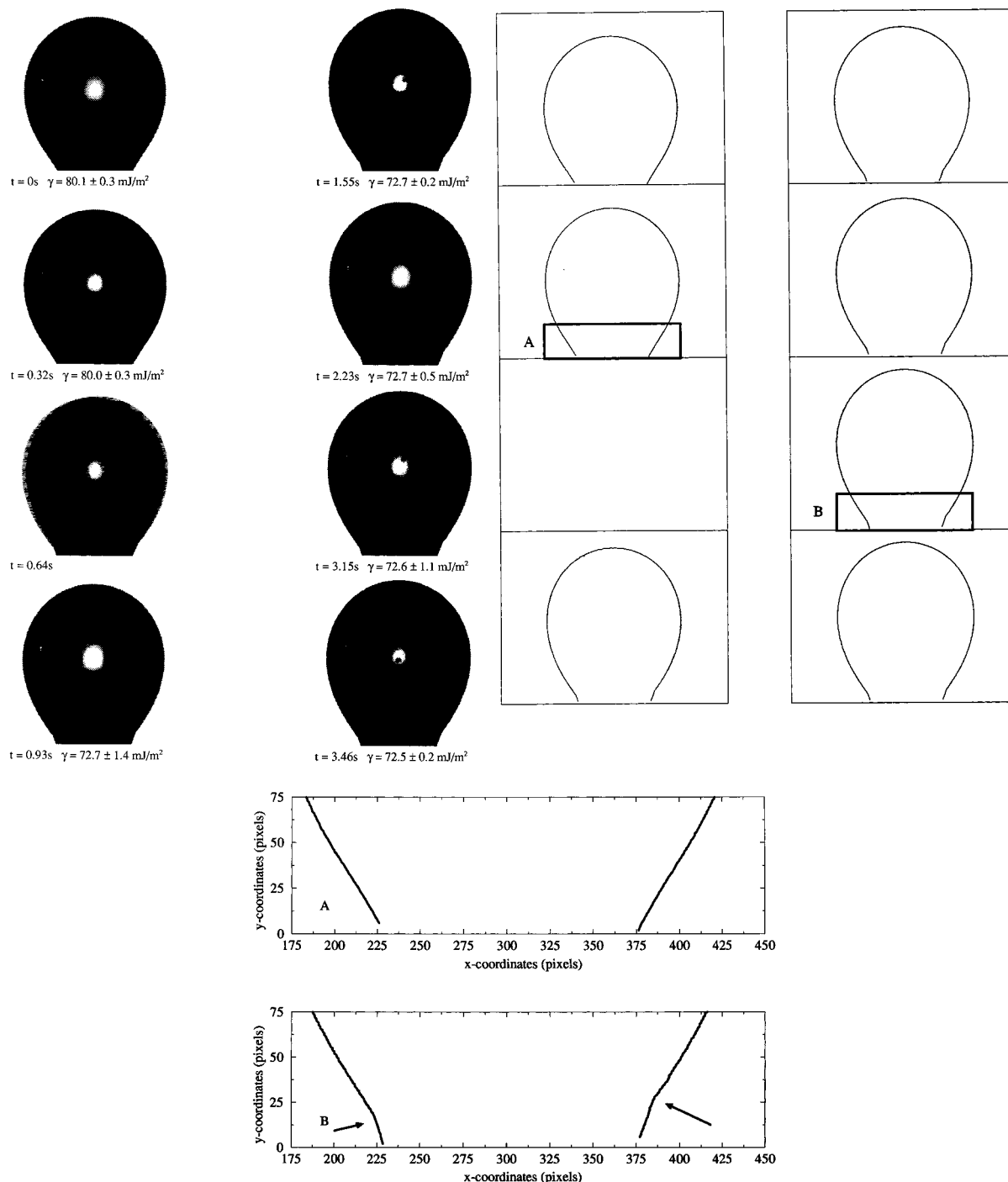


Figure 6. Consecutive images (a, left) of an air bubble showing the hexadecane film rupture at $t = 0.64\text{ s}$. Before film rupture, the tension is approximately 80.0 mJ/m^2 ; after film rupture, the tension is approximately 72.6 mJ/m^2 . The former represents film tension and the latter interfacial tension; the error limits associated with each tension value represent 95% confidence limits. The image at $t = 0.64\text{ s}$ is blurred due to vibration accompanying film rupture, and hence it cannot be analyzed by ADSA (b, right). The neck regions of images at $t = 0.32$ and 3.15 s are magnified in (c, bottom), where a smooth profile is seen for the bubble with film (A), but kinks appear after film rupture (B).

rate in Figure 7 differs from those in Figures 8 and 9 by almost an order of magnitude while the ratio of film tension to surface area remains roughly the same.

3. Interfacial Tensions. To measure interfacial tension between air and water, the capillary was placed into the water phase before the alkane was carefully added on the top of the water. This eliminated the possibility for alkane to come in contact with the tip of the Teflon tube and hence prevented the possibility of film formation. The air–water interfacial tension was measured on an air bubble formed at the tip of the Teflon tube, resulting in a value of $72.73 \pm 0.01\text{ mJ/m}^2$ at the 95%

confidence level (Table 1). This value is close to that observed after film rupture in Figures 5–9. The interfacial tensions between air and alkane and between water and alkane are also listed in Table 1. It is observed that the sum of the interfacial tensions between air and hexadecane and between hexadecane and water is approximately equal to the film tension.

B. Dodecane–Water. To support the observations with the hexadecane–water system, a second alkane, dodecane, was used for similar experiments. In the static measurement, when there was a film at the air–water interface, a smooth air bubble profile was observed. The resulting film tension was 77.20 ± 0.02

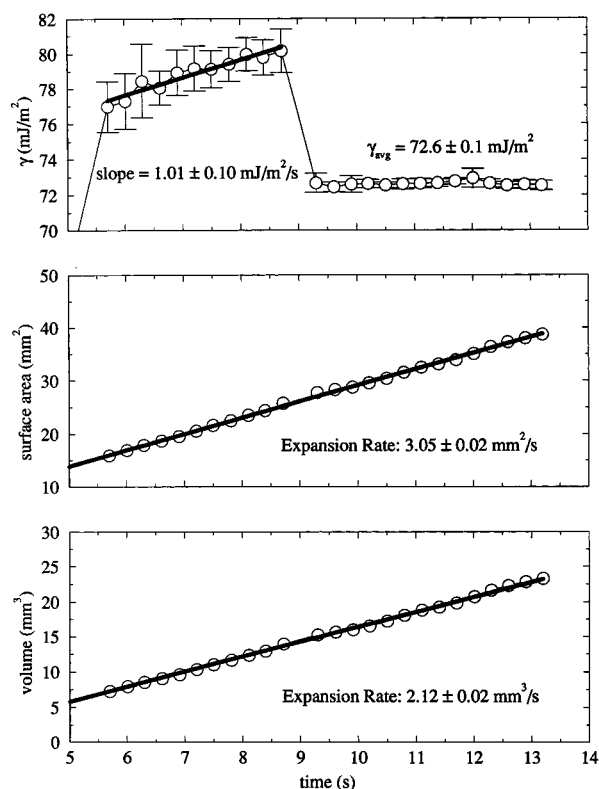


Figure 7. Dynamic tension measurement for the hexadecane–water system; the air bubble surface area is increased at a rate of $3.05 \pm 0.02 \text{ mm}^2/\text{s}$, corresponding to a volume increase at a rate of $2.12 \pm 0.02 \text{ mm}^3/\text{s}$. (The errors represent the standard deviations from the linear regression procedure.) An approximately 7.4 mJ/m^2 sudden drop in tension accompanies film rupture. A linear curve fit to the tension values before film rupture is also shown.

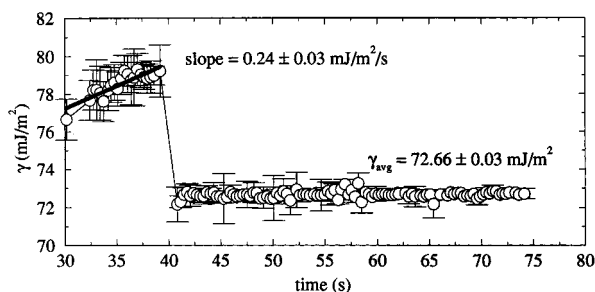


Figure 8. Dynamic tension measurement for the hexadecane–water system, similar to that in Figure 7, except that the air bubble surface area is increased at a rate of $0.61 \pm 0.01 \text{ mm}^2/\text{s}$, corresponding to a volume increase at a rate of $0.44 \pm 0.01 \text{ mm}^3/\text{s}$. The decrease in tension accompanying film rupture is again 7.4 mJ/m^2 .

mJ/m^2 at the 95% confidence level (Table 1). When there was insufficient alkane to form a film at the air–water interface, two kinks occurred in the neck region of the cross-section profile of the air bubble as before, due to formation of a “ring” of alkane at the base. The resulting surface tension was $72.61 \pm 0.01 \text{ mJ/m}^2$ at the 95% confidence level (Table 1).

Figure 10 shows the tension behavior as a function of time when the surface area is increased at three different rates: 1.04, 0.90, and $0.84 \text{ mm}^2/\text{s}$. In general, the same pattern as before is observed for all three expansion rates: an initial gradual increase in tension up to about 76.0 mJ/m^2 and then film rupture, resulting in a sharp decrease in the tension value to about 72.0 mJ/m^2 , which is close to the surface tension of water. Accompanying film rupture, the air bubble profile changes from smooth to kinked, due to formation of an alkane ring, as

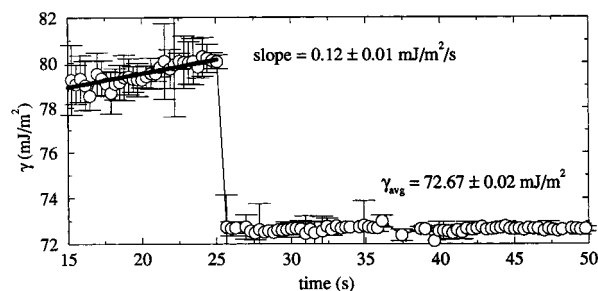


Figure 9. Dynamic tension measurement for the hexadecane–water system, similar to that in Figure 7, except that the air bubble surface area is increased at a rate of $0.52 \pm 0.02 \text{ mm}^2/\text{s}$, corresponding to a volume increase at a rate of $0.36 \pm 0.01 \text{ mm}^3/\text{s}$. The tension decrease upon film rupture is also 7.4 mJ/m^2 .

TABLE 1: Interfacial Tension and Film Tension (in mJ/m^2) from Static Measurements^a

interface	hexadecane	dodecane
air–water	72.73 ± 0.01	72.61 ± 0.01
air–alkane	27.23 ± 0.01	23.68 ± 0.01
alkane–water	53.53 ± 0.01	52.39 ± 0.01
(air–alkane) + (alkane–water)	80.76 ± 0.02	76.07 ± 0.02
alkane film on water	80.67 ± 0.06	77.20 ± 0.02

^a The sum of the interfacial tensions between air and alkane and between alkane and water is approximately equal to the alkane film tension. The error limits are at the 95% confidence level. The experimental temperature was $25 \pm 0.2 \text{ }^\circ\text{C}$.

illustrated in Figure 6. It is noted that with the slowest surface expansion rate a change in slope occurs at a tension value of 76 mJ/m^2 (Figure 10c). After this break, the tension value increases more slowly up to about 77 mJ/m^2 , close to the static film tension value, before film rupture. The ratios of the average rate of increase of film tension to the rate of surface expansion are again similar for all three area increase rates.

The surface (or interfacial) tensions between air and dodecane and the interfacial tension between dodecane and water were also measured just as for the hexadecane–water system; the results are presented in Table 1. It is noted that the sum of the surface tension between air and dodecane and the interfacial tension between dodecane and water is approximately equal to the dodecane film tension (Table 1).

IV. Discussion

The results show several features that are, as yet, not completely understood. The main point of course is the fact that the observed film tension is approximately equal to the sum of water–alkane interfacial tension and alkane surface tension. This finding is not surprising within the framework of well-established thinking. Relevant equations by Derjaguin and Gutop,^{25,26} Ivanov and Kralchevsky,²³ and de Feijter⁸ can be readily collapsed into²⁴

$$\gamma_f = \gamma_1 + \gamma_2 + O(\pi h) \quad (1)$$

where γ_f is the film tension, γ_1 and γ_2 are the two interfacial tensions, π is the disjoining pressure of the film, h is the thickness of the film, and O stands for the order of magnitude. If the disjoining pressure is negligible, the film tension should be just the sum of the two interfacial tensions. This is precisely the case for hexadecane, where, for the static measurements, $\gamma_f = 80.67 \pm 0.06 \text{ mJ/m}^2$, whereas $\gamma_1 + \gamma_2 = 80.76 \pm 0.02 \text{ mJ/m}^2$. Matters are quite different for the water–dodecane system, where $\gamma_f = 77.20 \pm 0.02 \text{ mJ/m}^2$, whereas $\gamma_1 + \gamma_2 = 76.07 \pm 0.02 \text{ mJ/m}^2$. The difference of about 1.1 mJ/m^2 will, presum-

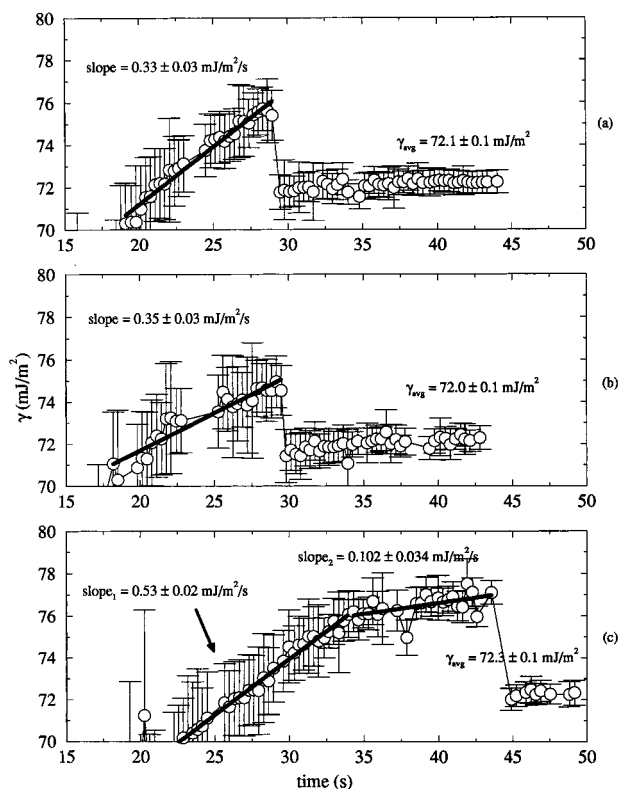


Figure 10. Dynamic tension measurement for the dodecane–water system, similar to that in Figure 7; the air bubble surface area is increased at a rate of (a) 1.04 ± 0.01 , (b) 0.90 ± 0.03 , and (c) 0.84 ± 0.02 mm²/s. Film rupture is accompanied by drop in tension of approximately 4.0 mJ/m². A linear curve fit to the tension values before film rupture is also shown in (a) and (b). In (c) a change in slope occurs at about 76 mJ/m², and two linear curve fits to the two branches are shown.

ably, have to be attributed to disjoining pressure effects. If this is indeed the case, the disjoining pressure would be positive; i.e., repulsion would occur. It is well-known, from statistical thermodynamics,²⁷ that the disjoining pressure is negative if only van der Waals forces are operative. However, in the present case, because of the presence of water, more complex responses, including repulsion, cannot be excluded a priori.

The differences between the results of the static and dynamic measurements also require comment. In the static measurements the bubble was formed relatively quickly and allowed to equilibrate for approximately 5 min before measurements were made. During this time film drainage will presumably have occurred until a metastable equilibrium state was reached. The static measurements are believed to represent such equilibria. In the dynamic measurements data acquisition was started as soon as the bubble, growing with a constant volume flow rate, was big enough to allow interpretation by ADSA-P. It is believed that the increase in tension as the film is thinning is not necessarily a disjoining pressure effect, since, in the majority of cases, these dynamic values are less than the sum of the two interfacial tensions. This effect could be due to the fact that the films are initially quite thick, and of uneven thickness, as sketched in Figure 11. The resulting tension exerted along the thick alkane layer is the vectorial sum of the two bounding surface tensions. If the two surface tension vectors (along the surfaces) are not parallel, the sum of the vectors will be less than the simple addition of their absolute values. As a result, a relatively low “film” tension value is obtained initially. As the alkane layer becomes thinner with the increase in the surface area, the film thickness will become more uniform. Eventually,

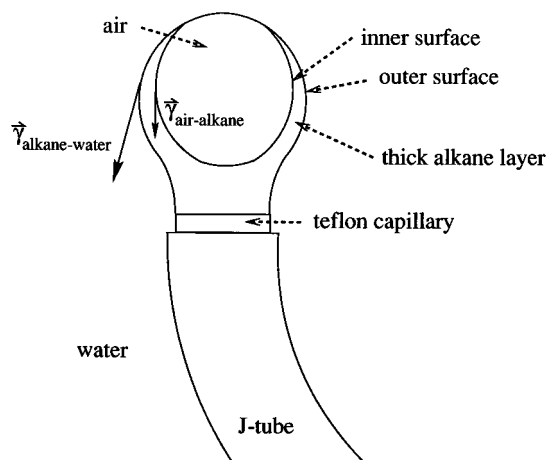


Figure 11. Schematic of a thick alkane layer on an air bubble with a relatively small surface area at the beginning of an expansion experiment. The two surface tension vectors, of the inner and outer surfaces of the alkane layer, are not in parallel, resulting in a smaller total tension value than the sum of water–alkane interfacial tension and alkane surface tension.

the alkane layer becomes thin enough that the two bounding surfaces become parallel; i.e., the alkane film has a constant film thickness everywhere on the surface. The film tension is then the sum of the two surface tensions, i.e., $\gamma_f = \gamma_1 + \gamma_2$, provided that the film is still thick enough so that there are no disjoining pressure effects. Unfortunately, the film ruptures in the majority of cases before this point is reached. In the static measurement, on the other hand, rupture occurs much later. The reason for this is presumably that natural drainage of the film is a much gentler process than the forced drainage due to film expansion. It is interesting that, in a single case, for dodecane (Figure 10c) the dynamic value of the tension exceeds the sum of γ_1 and γ_2 . A break in the γ values, just above 76 mJ/m² ($\gamma_1 + \gamma_2 = 76.07$ mJ/m²), occurs, and the slope of the subsequent data may contain information about disjoining pressure and film thickness.

Finally, there is one more feature of the data that requires comment: Error limits are significantly larger in the presence of films than in their absence. There is no obvious explanation for this fact. Speculation that fluid dynamic processes in the film could cause temporal distortions in the drop shape is probably not correct. Our basic measuring stick is the pixel, which, in these experiments, is approximately 10 μ m. It seems unlikely that such dynamic effects could have amplitudes well in excess of this length.

Comparison with Other Film Tension Methods. As mentioned in the Introduction, only a small number of methods^{9–18} have been developed for measuring film tension. All of these approaches make use of a spherical drop or bubble and relate the simple geometric parameters of the sphere to the Laplace equation of capillarity to calculate film tension. Platanov et al.^{14,16} reported an experimental method for direct measurement of the film tension of black foam films. Their foam films are obtained in the form of a spherical semibubble, whose radius of curvature is determined from microphotographs and the capillary pressure is measured by a manometer. The film tension is calculated from these data by using the Laplace equation of capillarity. This method is applied only to foam films that are bounded by two adjacent gaseous phases.

Another method for measuring film tension that has since emerged^{17,18} is not restricted to foam films; the bounding phases can also be liquid. In the experiment, a single liquid drop coated

with a film is formed at the tip of a capillary, and the capillary pressure in the drop is measured. The film tension is calculated from the capillary pressure and the film radius of curvature by using the Laplace equation of capillarity. However, to use this method, the drop supporting the film must be spherical in shape. This, therefore, limits the use of this technique.

The present method circumvents these difficulties. The bounding phase can be either liquid or gas, which is useful for many three-phase systems involving gas and liquids, such as in oil production where water, oil, and gaseous phases often coexist.^{28,29} With the present method, the drop or bubble shapes do not have to be spherical as long as they are axisymmetric; hence, the Eötvös number does not have to be controlled to be under 0.02.¹⁷ In addition, this method has the ability to perform film tension measurements under both static and dynamic conditions, and information about the surface area, drop, or bubble volume and the radius of curvature can all be obtained simultaneously.

V. Conclusions

1. From both static and dynamic experiments, the observed exceedingly high tension value is that of an alkane film at the air–water interface.

2. Film tensions of hexadecane and dodecane on the air–water interface are found to be 80.67 ± 0.06 and 77.20 ± 0.02 mJ/m², respectively, at the 95% confidence level, at a temperature of 25 ± 0.2 °C.

3. The alkane film tension found is roughly equal to the sum of the interfacial tensions of air–alkane and of alkane–water for both hexadecane– and dodecane–water systems. In the case of dodecane, the static film tension as well as a single dynamic value are larger than the sum of the two interfacial tensions, possibly indicating disjoining pressure effects.

4. Film rupture has been shown in the abrupt change in the air bubble image as well as in the sudden decrease in the tension value. Before film rupture, the film tension measured increases with the increase in surface area, and the ratio of the tension increase rate to the surface expansion rate is independent of the surface expansion rate. This indicates that the dynamic film tension is related only to the film thinning.

5. The method presented provides a new approach to film tension measurement, which requires only axisymmetric bubble shapes, rather than spherical ones. The measurements can be carried out under both static and dynamic conditions.

Acknowledgment. This research was supported by the Natural Sciences and Engineering Research Council of Canada (Grant A8278) and an Ontario Graduate Scholarship (P.C.).

References and Notes

- (1) Adamson, A. W. *Physical Chemistry of Surfaces*, 5th ed.; John Wiley & Sons: New York, 1990; Chapter 4.
- (2) Kwok, D. Y.; Hui, W.; Lin, R.; Neumann, A. W. *Langmuir* **1995**, *11*, 2669.
- (3) Rotenberg, Y.; Boruvka, L.; Neumann, A. W. *J. Colloid Interface Sci.* **1983**, *93*, 169.
- (4) Cheng, P.; Li, D.; Neumann, A. W. *Colloids Surf.* **1990**, *43*, 151.
- (5) Cheng, P.; Neumann, A. W. *Colloids Surf.* **1992**, *62*, 297.
- (6) Lahooti, S.; del Río, O. I.; Cheng, P.; Neumann, A. W. In *Applied Surface Thermodynamics*; Neumann, A. W., Speltz, J. K., Eds.; Marcel Dekker: New York, 1996; Chapter 10.
- (7) Chen, P.; Kwok, D. Y.; Prokop, R. M.; del Río, O. I.; Susnar, S. S.; Neumann, A. W. In *Drops and Bubbles in Interfacial Research*; Möbius, D., Miller, R., Eds.; Elsevier: Amsterdam, The Netherlands, 1997; Chapter 2.
- (8) de Feijter, J. A. In *Thin Liquid Films*; Ivanov, I. B., Ed.; Marcel Dekker: New York, 1988; Chapter 1.
- (9) Mysels, K. J.; Huisman, H. F.; Razouk, R. *J. Phys. Chem.* **1966**, *70*, 1339.
- (10) Huisman, H. F.; Mysels, K. J. *J. Phys. Chem.* **1969**, *73*, 489.
- (11) Kolarov, T.; Scheludko, A.; Exerovova, D. *Trans. Faraday Soc.* **1968**, *64*, 2864.
- (12) Princen, H. M.; Frankel, S. J. *Colloid Interface Sci.* **1971**, *35*, 386.
- (13) de Feijter, J. A.; Vrij, A. *J. Colloid Interface Sci.* **1978**, *64*, 269.
- (14) Platikanov, D.; Nedyalkov, M.; Rangelova, N. *Colloid Polym. Sci.* **1987**, *265*, 291.
- (15) Nedyalkov, M.; Schoppe, G.; Platikanov, D. *Colloids Surf.* **1990**, *47*, 95.
- (16) Platikanov, D.; Nedyalkov, M.; Rangelova, N. *Colloid Polym. Sci.* **1991**, *269*, 272.
- (17) Soos, J. M.; Koczko, K.; Erdos, E.; Wasan, D. T. *Rev. Sci. Instrum.* **1994**, *65*, 3555.
- (18) Nagarajan, R.; Koczko, K.; Erdos, E.; Wasan, D. T. *AIChE J.* **1995**, *41*, 915.
- (19) Princen, H. M.; Mason, S. G. *J. Colloid Interface Sci.* **1965**, *29*, 156.
- (20) Holcomb, C. D.; Zollweg, J. *J. Colloid Interface Sci.* **1990**, *134*, 41.
- (21) Mysels, K. J. *Colloids Surf.* **1990**, *43*, 241.
- (22) Susnar, S. S.; Hamza, H. A.; Neumann, A. W. *Colloids Surf. A: Physicochem. Eng. Aspects* **1994**, *89*, 169.
- (23) Ivanov, I. B.; Kralchevsky, P. A. In *Thin Liquid Films*; Ivanov, I. B., Ed.; Marcel Dekker: New York, 1988; Chapter 2.
- (24) Chen, P. Ph.D. Thesis, University of Toronto, Toronto, Ontario, Canada, in preparation.
- (25) Derjaguin, B. V.; Gutop, Yu. V. *Colloid J. USSR* **1965**, *27*, 574; *Kolloidn. Zh.* **1965**, *27*, 674.
- (26) Derjaguin, B. V.; Gutop, Yu. V. In *Research in Surface Forces*; Derjaguin, B. V., Ed.; Consultants Bureau: New York, 1966; Vol. 2, pp 17–22.
- (27) Nir, S.; Vassilieff, C. S. In *Thin Liquid Films*; Ivanov, I. B., Ed.; Marcel Dekker: New York, 1988; Chapter 4.
- (28) Rossen, W. R. In *Foams*; Prud'homme, R. K., Khan, S. S., Eds.; Marcel Dekker: New York, 1996; Chapter 11.
- (29) Princen, H. M. *J. Colloid Interface Sci.* **1997**, *187*, 520.